Electrochemical Behaviour and Interfacial Contact Resistance of Ti-6Al-4V and SUS 316L plates with Potential Application as a Bipolar Plate in PEMFC

Nur Fawwaz Asri[*]*, T. Husaini, Edy Herianto Majlan*
Fuel Cell Institute, Universiti Kebangsaan Malaysia,
43600 UKM Bangi, Selangor, Malaysia.
[*]*nurfawwazasri@ymail.com*

Abu Bakar Sulong
Department of Mechanical and Material Engineering,
Faculty of Mechanical and Build Environment,
Universiti Kebangsaan Malaysia, 43600 UKM Bangi, Selangor, Malaysia.

Wan Ramli Wan Daud
Department of Chemical and Process Engineering,
Faculty of Mechanical and Build Environment,
Universiti Kebangsaan Malaysia, 43600 UKM Bangi, Selangor, Malaysia.

ABSTRACT

The main aim of this study is to investigate the corrosion of Ti-6Al-4V and SUS 316L plates as application at anode and cathode condition in PEMFC. The criteria for both current density (<1 μA cm^{-2}) and interfacial contact resistance (<10 mΩ cm^2) must meet the DOE's 2020 technical targets. In approaching a lightweight and ease of manufacture bipolar plates, both selected materials were chosen based on their good and relatively low cost factor compared to graphite. Corrosion resistance were observed for both plates as preparation for long-term operations in PEMFC. Potentiostatic test measurements were carried out at room temperature in a solution of 0.5 M H_2SO_4 with a scan rate 10 mV/s for 10 hours. The result shows good performance of SUS 316L corrosion resistance as compared to Ti-6Al-4V, but it still does not achieve the DOE target. To provide high corrosion resistance at cathode as well as increasing electrical conductivity at anode in PEMFC components, Cr was proposed as surface modification on plates.

ISSN 1823- 5514, eISSN 2550-164X
Received for review: 2017-04-25
Accepted for publication: 2017-06-05
Published: 2017-08-15

The current density and ICR decreased to 0.1 μA cm^{-2} and 17.6 mΩ cm^{2} for 12 hours immersed during potentiostatic test. Surface modification using PVD magnetron sputtering with 150 W and 80 minutes of deposition was successfully deposited and potentially as bipolar plates in PEMFC application.

Keywords: *Proton Exchange Membrane Fuel Cell (PEMFC), Ti-6Al-4V, SUS 316L, Corrosion Resistance, Interfacial Contact Resistance*

Introduction

Hydrogen could be the key in certain energy application in the future and will potentially be a replacement to fossil fuel as an energy storage medium because of its zero emission, low noise and high energy efficiency factors [1]. Many research projects have been carried out with the purpose to find cleaner way to produce hydrogen. In facts, most industries in Japan, Korea and Europe have already used and powered their vehicles without emitting harmful carbon dioxide responsible for global warming by using hydrogen energy [2]. Therefore, fuel cell power system using hydrogen energy has good potential for clean atmosphere and is efficient for transportation [2, 3]. Thus, it delivers more energy for every fuel and implies that a vehicle which uses hydrogen fuel will go a lot farther than a vehicle that has the same amount of traditional petrol [4].

Until now, fuel cell technology has been made to improve the proton exchange membrane fuel cell (PEMFC), as the bipolar plates contribute 60% – 80% of the total component in the PEMFC stack [5-7]. To develop and optimize more cost effective materials of bipolar plates, recent studies have moved from graphite to metals and composites. However, metallic bipolar plates possess excellent electrical conductivity, high strength, low gas permeability and can be manufactured at low cost instead of processed into thin plates [8].

This paper work focuses on the corrosion resistance and interfacial contact resistance of Ti-6Al-4V and SUS 316L with potential application as bipolar plate in PEMFC condition. Both metallic materials provide a good alternative as the bipolar plate requires fabrication of channels in the plate surfaces [9]. In addition, metallic materials have high ductility and ease of manufacturing processes especially for mass production compared to graphite [9, 10]. The material preparation is not complex as ceramic polymers bipolar plates because they are readily made materials [11]. Thus, titanium and stainless steel can be used to produce strong bipolar plates with inexpensive process fabrication. However, the corrosion process is a major concern when

using metallic bipolar plate which the corrosion rate is less than 100 mm/year [12].

Ti-6Al-4V and SUS 316L were suggested as the candidates for a metallic bipolar plate due to ease of machining process and ligthweight instead of good mechanical properties. The metallic plates were studied without any treatment process on the surface metal to observe the surface development from the formation of micro pores and micro cracks. In the real environment of PEMFC system, anode cell interacts as current collector where the hydrogen gas produces hydrogen ion before going through the cathode cell. In the PEMFC, oxidation occurs more on cathode cell because of oxygen reduction and high water concentration [13]. Due to this activity, PEMFC performance drops when the corrosion occurs more at the cathode eventhough electrical conductivity increases at the anode [7, 13]. In this study, electrochemical behavior of Ti-6Al-4V and SUS 316L plates are observed as bipolar plates potential in PEMFC condition.

Experimental

Materials and chemical composition

Materials used in this study were Ti-6Al-4V and SUS 316L as metal plates preparation for the bipolar plates in PEMFC. Table 1 shows nominal compositions of Ti-6Al-4V and SUS 316L plates. The samples of disk shaped (coupon) with a thickness of 2 mm were recommended. A lesser thickness will provide lightweight material to sustain with reasonable strength for the bipolar plates. Yuan et al. had reviewed the design criteria of bipolar plate for low weight and volume that can withstand high temperature in PEMFC operating system [5]. The coupon were ultrasonically cleaned in acetone for 30 minutes to remove any contaminants from the surface metals. The preparation procedure to get the ICR values and potentiodynamic polarisation test consisted of grinding coupon surfaces from 240, 320, 400 and 600 grit SiC papers, followed by polishing with 6 micron and 1 micron diamond suspension, respectively. The nominal composition showed that the major component in Ti-6Al-4V is Ti itself between 88–90 wt %, while SUS 316L plates consists of Cr and Ni with 16–18 wt% and 10–14 wt % each respectively. The nominal composition showed that the major component in Ti-6Al-4V is Ti itself between 88–90 wt %, while SUS 316L plates consists of Cr and Ni with 16–18 wt% and 10–14 wt % each respectively.

Table 1: Nominal composition of Ti-6Al-4V (Ti) and SUS 316L (SS) [14, 15].

Types of material **Element**	**Ti-6Al-4V** **wt %**	**SUS 316L** **wt %**
Carbon (C)	<0.10	<0.03
Manganese (Mn)	–	<2.00
Phosphorus (P)	–	<0.045
Sulfur (S)	–	<0.03
Silicon (Si)	–	<0.75
Chromium (Cr)	–	16.00–18.00
Nickel (Ni)	–	10.00–14.00
Molybdenum (Mo)	–	2.00–3.00
Nitrogen (N)	<0.05	<0.10
Iron (Fe)	<0.30	Balance
Aluminum (Al)	5.50–6.70	–
Vanadium (V)	3.50–4.50	–
Oxygen (O)	<0.20	–
Hydrogen (H)	<0.02	–
Titanium (Ti)	Balance	–

Interfacial Contact Resistance (ICR)

To get numeral values of the ICR, the measurement is determined by calculating both areas of piston and samples used during experiment, as in the form of Equation 1 and Equation 2. The diameter of the piston and metal plates were 40 mm and 20 mm, respectively. Areas and applied current:

$$A_{piston} = \pi r^2 \quad (1)$$

$$A_{sample} = \pi r^2 \quad (2)$$

Here, P denotes the pressure from the piston at 150 N/cm^2 onto the area of metal plates, in the text Equation 3. Force excited on plate:

$$F = P/A \quad (3)$$

The contact resistance were measured from potential (V) and current (A) resistance at 150 N/cm^2 (15 bar) which can be referred to in Equation 4. Contact resistance at 15 bar:

$$R = V/I \quad (4)$$

Hence, the ICR value for the metal plates denotes the resistance of the results obtained, Equation 5.

$$ICR = R(A_{sample}) \quad (5)$$

Observation was made for the ICR for the preferred parameter from temperature 40 °C to 80 °C. The current employed was 0.1 A to 1 A, respectively. The current (I) was sent through in a complete setup whereas the potential (V) was measured through a circuit in different preheating temperature of 40 ºC, 60 ºC and 80 ºC. Figure 1 shows the apparatus of interfacial contact resistance based on the ICR setup.

Figure 1: Interfacial contact resistance (ICR) apparatus.

Electrochemical cell by potentiodynamic polarization measurement

Electrochemical measurement was carried out on Radiometer Analytical equipment by potentiostat PGZ100 (Voltalab 10) as in Figure 2. The procedure was controlled by VoltaMaster 4 electrochemical software. A flat cell was used for the coupon at ambient temperature in a solution of 0.5 M H_2SO_4.

The coupon with 20 mm diameter was clamped to the flat cell and the surface mirror was exposed to the solution. The coupon was used as the working electrode, a saturated calomel electrode Ag/AgCl (SCE) was used as reference electrode and a platinum electrode acted as counter electrode. All potentials were referred to the SCE during the experiment. The sample was stabilized at open circuit potential (OCP) for 1 hour and then was polarized from OCP to positive direction with a scan rate of 10 mV/s.

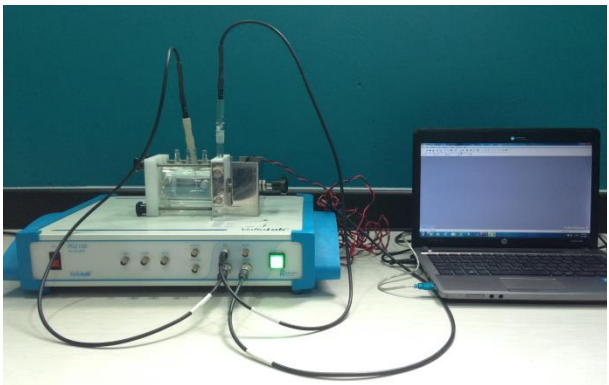

Figure 2: Experimental set-up for electrochemical measurement of Ti-6Al-4V and SUS 316L coupon samples using potentiostat PGZ100 (Voltalab 10).

Results and Discussion

Interfacial contact resistance of Ti-6Al-4V and SUS 316L plates at 40 °C – 80 °C.

The ICR values with current ranging from 0.1 A to 1 A for each sample were observed. Parameter with the current 1 A was chosen as the best graph pattern and lowest ICR amongst other values as in Table 2. The ICR values of Ti-6Al-4V plates ranged between 33.8 mΩ cm² to 25.6 mΩ cm² while SUS 316L plates ranged between 45.3 mΩ cm² to 29.8 mΩ cm². It was observed that lower potential at higher temperature gave low ICR values.

Table 2: The potential (V) and current (A) resistance for Ti-6Al-4V and SUS 316L between 40 °C to 80 °C at 1 A.

Material	**Ti-6Al-4V**			**SUS 316L**		
T (ºC)	**I (A)**	**V (mV)**	**ICR (mΩ cm²)**	**I (A)**	**V (mV)**	**ICR (mΩ cm²)**
40	1	2.2	33.8	1	2.9	46.3
60	1	2.0	30.7	1	2.3	36.1
80	1	1.6	25.6	1	2.0	29.8

The graph pattern in Figure 3 indicates stable performance of Ti-6Al-4V and SUS 316L plates ICR values against temperature. Both results show the ICR values decreased as the temperature increased from 40 °C to 80 °C. Nevertheless, the ICR of SUS 316L decreased sharply against temperature

compared to Ti-6Al-4V. The percentage at 40 °C was 31.2 % and it decreased to 15.2 % at 80 °C. It was reported that the influence of small amount temperature to the austenitic stainless steel containing much higher Cr and Ni elements (refer in Table 1) had reduced the ICR by increasing the temperature [16]. Overall, the Ti-6Al-4V obtained the lowest ICR value compared to SUS 316L. Nevertheless, both metallic plates did not achieve U.S Department of Energy (DOE) target for ICR value which is less than 10 mΩ cm².

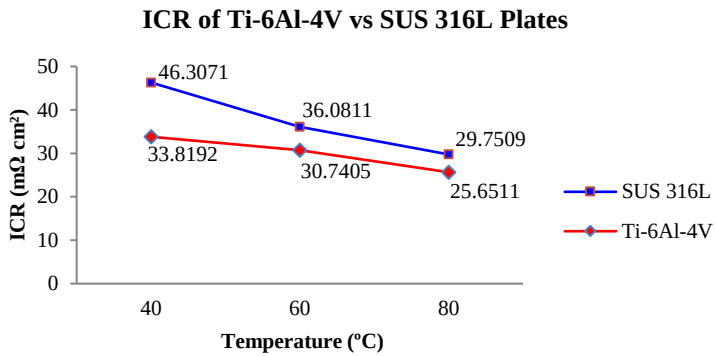

Figure 3: Interfacial contact resistance (ICR) of Ti-6Al-4V and SUS 316L plates over temperature (40 °C – 80 °C) at 1 A.

Corrosion behavior of Ti-6Al-4V and SUS 316L plates towards Graphite plates

Potentiodynamic polarization measurement was used to determine the active-passive characteristics of Ti-6Al-4V and SUS 316L in different concentrations of 0.5 M H_2SO_4 solution. The clamped coupons only exposed 10 mm diameter area (in circle and red fit) as shown in Figure 4. Figure 5 represents polarization curves of Ti-6Al-4V and SUS 316L in comparison with corrosion behaviour of graphite. According to Figure 5, the initial OCP values for Ti-6Al-4V, SUS 316L and graphite were -810 mV, -2560 mV and -1264 mV (Ag/AgCl) in H_2SO_4 solution. This value turned into a passive state after less than 3600 s. The Ti-6Al-4V plate was in passive state under test condition from -300 to 900 mV, while SS plate could be passivated spontaneously under the same condition from -1200 to 1600 mV versus SCE for 10 hours. The I_{corr} Ti-6Al-4V and SUS 316L were 300 µA/cm² and 4.9 µA/cm², respectively. Both metal plates in the potential range of -2000 to 4000 mV (SCE) at room temperature have similar general features but SUS 316L exhibited much better corrosion resistance, in accordance with the result of the corrosion potential experiment.

In comparison, graphite plate in the potential range of -2000 to 4000 mV had passivation state starting from -1200 to 38 mV and the I_{corr} recorded was 7.3 µA/cm^2, respectively. The result shows that large passivation area totally increases corrosion resistance of material. It was observed that the passivation helps to delay the corrosion process before trans-passivation behaviour rapidly increase to the anodic region.

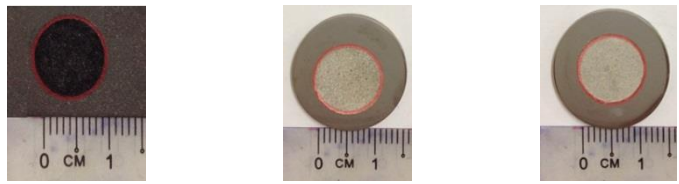

(a) Graphite (b) Ti-6Al-4V (c) SUS 316L

Figure 4: Macrostructure observation for the untreated samples (a) graphite (b) Ti-6Al-4V and (c) SUS 316L with 10 mm surface area exposed in 0.5 M H_2SO_4 after 10 hours of potentiodynamic polarisation test.

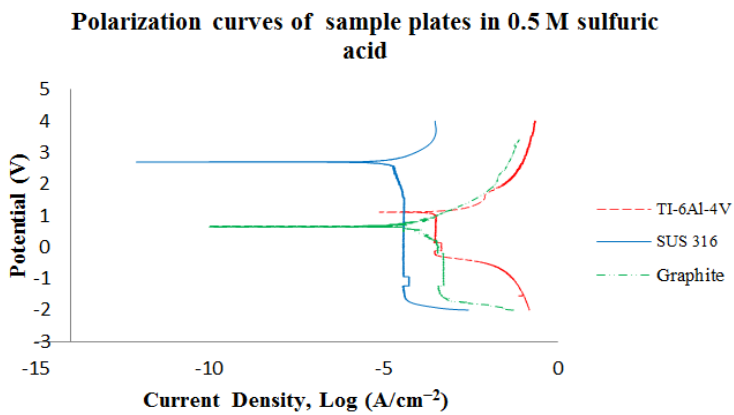

Figure 5: Polarization curves of untreated samples in 0.5 M H_2SO_4 solutions at room temperature with a scan rate of 10 mVs^{-1}.

Potential (E_{corr}), current density (I_{corr}), anodic and cathodic Tafel slopes and corrosion rates (CR) are presented in Table 3. It is observed that Ti-6Al-4V has very poor resistant to corrosion compared to SUS 316L. The values of the I_{corr} at any given temperature are higher for Ti alloy and exhibits higher thickening rate for its oxide film growth as compared to SS and

graphite [3, 17]. Some authors considered Mo element in some Ti alloy for the improvement of the mechanical properties and to increase the corrosion resistance [3, 18, 19], whereas Ti-6Al-4V type has no element of Mo and Ni. As listed in Table 3, the highest E_{corr} is 2700 mV which is produced by SUS 316L. It can be observed that by increasing the E_{corr} value, the I_{corr} value will decrease and potentially reduce the corrosion attack, as low as SUS 316L at 4.9 µA / cm^2. Rockwell hardness test was intended at three regions of the plates before corrosion test. The highest hardness average value was recorded by Ti-6Al-4V at 31.9 HRC, while 22.2 HRC was recorded for SUS 316L. Higher hardness value does not necessarily indicate good corrosion resistance. Nevertheless, graphite was used as bipolar plates because of its low surface contact resistance and high corrosion resistance, but brittle and permeable to gases with poor cost effectiveness for high volume manufacturing processes [20].

Table 3: The electrochemical parameters and hardness properties of Ti-6Al-4V, SUS 316L and graphite.

Plate	**E_{corr} (mV)**	**I_{corr} (µA / cm^2)**	**Tafel Slopes (mV)**		**CR (µm/year)**
			ß$_a$	**ß$_c$**	
Ti-6Al-4V	1100.0	300.0	132.6	-54.9	13500
SUS 316L	2700.0	4.9	147.6	-185.7	207.7
Graphite	600.0	7.3	66.8	-133.0	64.42

The composition analyses by Energy Dispersive X-ray (EDX) are presented in Figure 6. The Cr and Ni element in SS were main passive components of the passive step in the anodic polarization that was able to reduce corrosion rate and current density, and Mo was known to increase the resistance to localized and pitting corrosion [21, 22].

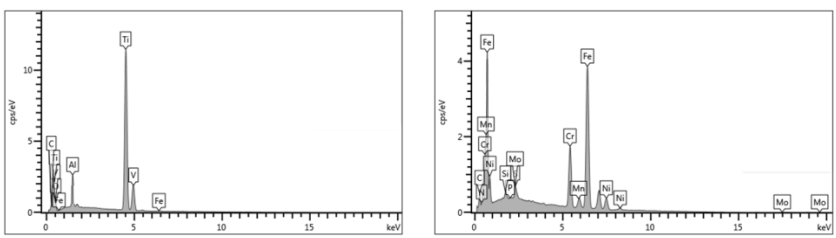

(a) Ti-6Al-4V (b) SUS 316L

Figure 6: EDX showing the elements present in untreated sample plates of (a) Ti-6Al-4V and (b) SUS 316L.

Morphology surface of corrosion analysis

SEM surface morphology analysis results for Ti-6Al-4V are shown in Figure 7. The solid surface of Ti-6Al-4V was activated by immersion in H_2SO_4 solution and small sized pore was created, as shown in Figure 7(a). These pores contained a mixture of air, (but depleted to some extent of oxygen), arising from the H_2SO_4 solution [23]. Upon immersion, deep pores were created on the oxide layer through the grain structure. The porosity in Figure 7(b) was magnified from the located position. It created small pits which did not propagate into large ones. The roughness and loss of weight of the immersed area increased as macrostructure observed in Figure 4(b), due to the localized attack .

Typical corrosion morphology was different for SUS 316L. From the results in Figure 8(a), the oxide layer existed with the beginning of pore creation delayed occurring after anodization compared to Ti-6Al-4V. In contrast, Figure 7(b) has deeper pores with rapid oxidation process through the grain surface as shown by '1', while Figure 8(b) has an irregularly shaped pit continued to develop along the grain surface as shown by '2'. Hence, the enlargement of SUS 316L grain size reacted against temperature, which is discussed in Figure 3. Therefore, this statement is supported by the references in Figure 6, whereas Cr and Ni element in SS are able to reduce corrosion rate while Mo element increases the resistance to localized and pitting corrosion.

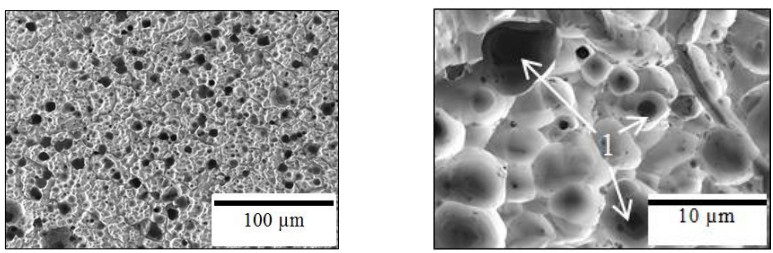

(a) (b)

Figure 7: SEM surface morphology images of (a) Ti-6Al-4V after polarization test (b) is magnified from the located position as shown by '1'.

The concentrations of Ti, Al, and O elements in Ti-6Al-4V were distributed relatively uniformly around the pitting regions after potentiodynamic polarization test [24]. It was clearly observed that the oxidation process further occurred homogeneously to gradually strengthen the corrosion upon pitting nucleation and rapid loss of weight as in Figure 4 (b) respectively. Based on the review, occurrence of pitting initiation for metal plates usually occurs on MnS inclusions and/or oxide inclusion [25].

Due to the assumption, the pit morphology was changed from round to irregular shape for SUS 316L (Figure 8) because it has all elements which will help the pit to be initiated.

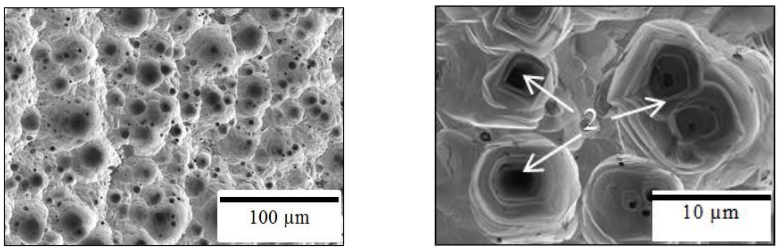

(a) (b)

Figure 8: SEM surface morphology images of (a) SUS 316L after polarization test (b) is magnified from the located position as shown by '2'.

ICR and corrosion resistance of 316L plates after Cr surface modification

Surface modification using PVD magnetron sputtering with 150 W and 80 minutes of deposition was successfully deposited on Cr-coated SUS 316L plates. The ICR with the current of 1 A for SUS 316L before and after surface modification with Cr were observed. The ICR were measured at temperature 40 ºC, 60 ºC and 80 ºC respectively. The ICR values decreased as the temperature increased from 40 °C to 80 °C. The improvements were observed after coating from 29.8 mΩ cm² to 17.6 mΩ cm².

Nonetheless, the graph pattern of SUS 316L decreases sharply against temperature as compared to Cr-coated sample. Difference similarities percentages between SUS 316L and Cr-coated sample at 40 °C were 75 % and it decreased to 51 % at 80 °C. It was reported that the influence of small amount temperature to the austenitic stainless steel containing much higher Cr and Ni elements had reduced the ICR by increasing the temperature [16]. Thus, Cr-coated sample obtained lower ICR value after surface modification.

Table 4: The potential (V) and current (A) resistance for SUS 316L and Cr-coated between 40 °C to 80 °C at 1 A.

Material	**SUS 316L**			**Cr-coated**		
T (ºC)	**I (A)**	**V (mV)**	**ICR (mΩ cm²)**	**I (A)**	**V (mV)**	**ICR (mΩ cm²)**
40	1	2.9	46.3	1	1.3	21.0
60	1	2.3	36.1	1	1.2	20.6
80	1	0.2	29.8	1	1.1	17.6

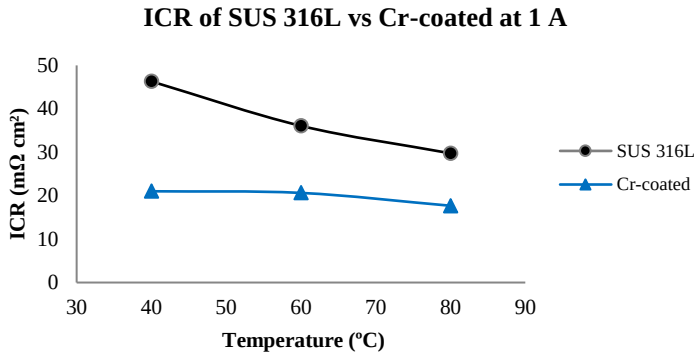

Figure 9. Interfacial contact resistance (ICR) of SUS 316L and Cr-coated plates over temperature (40 °C – 80 °C) at 1 A.

To evaluate the improvisation of corrosion resistance after Cr surface modification on 316L plates, the potentiodynamic polarization test results are shown in Table 5.

In comparison, SUS 316L showed higher corrosion densities and higher corrosion potential readings. Cr coatings protect SUS 316L plates efficiently which recorded 0.1 µA cm^{-2} at 2593 mV (SCE), respectively. Cr coatings are good candidate for SUS 316L plates. It is supported by polarization curves results in Figure 10. The increase of corrosion current density in anodic branch was slower for Cr-coated plates than SUS 316L plates. It was observed that the corrosion attack happened due to the increase of current densities. The scan rate of 10 mV s^{-1} for Cr-coated extended from 10 hours to 12 hours after the corrosion attack stopped.

Table 5: The electrochemical parameters of SUS 316L before and after Cr-coated.

Plate	E_{corr} (mV)	I_{corr} (µA / cm^2)	Tafel Slopes (mV)		CR (µm/year)
			$ß_a$	$ß_c$	
SUS 316L	2700.0	4.9	147.6	-185.7	207.7
Cr-coated	2593.0	0.1	45.7	-47.8	5.783

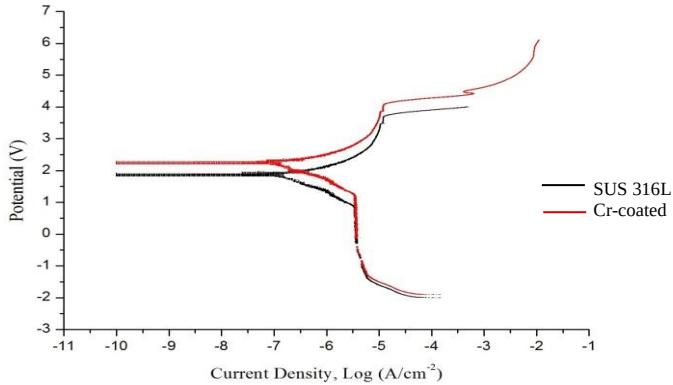

Figure 10: Polarization curves of SUS 316L and Cr-coated plates in 0.5 M H_2SO_4 solutions in comparison.

Conclusion

The potentiodynamic polarization tests showed good performance of corrosion resistance in SUS 316L as compared to Ti-6Al-4V. However, the I_{corr} still did not achieve the DOE target of <1 µA/cm^2. To sustain higher electrical conductivity at anode thus providing high corrosion resistance <1 µA/cm^2 at cathode in a real PEMFC condition, the findings of this research suggest the following conclusions:

1. The ICR values for both metallic plates decrease when temperature increase. However the ICR of austenitic SUS 316L drastically responds against temperature in comparison with Ti-6Al-4V. The I_{corr} of Ti-6Al-4V increased to 300 µA/cm^2, displacing E_{corr} towards less noble potential at 1100 mV, which makes less passivation to give poor corrosion resistance. On the other hand, Cr, Ni and Mo elements help to improve the mechanical properties and corrosion resistance in choosing SUS 316L as bipolar plates materials.
2. Cr and Ni elements were able to reduce corrosion rate while Mo element increased the resistance to localized and pitting corrosion. Still, existing pits from the corrosion attack were present from round to irregular shape for SUS 316L with reducing the oxidation process. For that reason, different coating materials at anode and cathode bipolar plates were proposed as improvements to achieve the DOE target.

Acknowledgement

This research was funded by 2014 GGPM Grants Research Project and LRGS/2013/UKM-UKM/TP-01, as well as Ministry of Higher Education for the financial support during the research studies. The authors gratefully acknowledge everyone who provide valuable suggestions and collaboration in this research. Special thanks to Associate Prof. Dr. Bushroa Abdul Razak and Faculty of Engineering, University of Malaya for their greatest support in the coating of metal bipolar plates.

References

[1] S.E. Hosseini, M.A. Wahid, "Hydrogen production from renewable and sustainable energy resources: Promising green energy carrier for clean development", *Renewable and Sustainable Energy Reviews*, 57, 850-866, (2016).

[2] A.F. Ambrose, A.Q. Al-Amin, R. Rasiah, R. Saidur, N. Amin, "Prospects for introducing hydrogen fuel cell vehicles in Malaysia", *International Journal of Hydrogen Energy*, 42, 9125-9134, (2016).

[3] J.-J. Hwang, "Sustainability study of hydrogen pathways for fuel cell vehicle applications", *Renewable and Sustainable Energy Reviews*, 19, 220-229, (2013).

[4] R.A. Huggins, Hydrogen Storage, *Energy Storage*, Springer, 95-118, (2016).

[5] X.Z. Yuan, H. Wang, J. Zhang, D.P. Wilkinson, "Bipolar plates for PEM fuel cells-from materials to processing", *Journal of New Materials for Electrochemical Systems*, 8, 257, (2005).

[6] D. Zhang, Z. Wang, K. Huang, "Composite coatings with in situ formation for Fe–Ni–Cr alloy as bipolar plate of PEMFC", *International Journal of Hydrogen Energy*, 38, 11379-11391, (2013).

[7] N.F. Asri, T. Husaini, A.B. Sulong, E.H. Majlan, W.R.W. Daud, "Coating of stainless steel and titanium bipolar plates for anticorrosion in PEMFC: A review", *International Journal of Hydrogen Energy*, 42, 9135-9148, (2016).

[8] R. Taherian, "A review of composite and metallic bipolar plates in proton exchange membrane fuel cell: Materials, fabrication, and material selection", *Journal of Power Sources*, 265, 370-390, (2014).

[9] K.S. Lyons, B.D. Gould, "Lightweight titanium metal bipolar plates for PEM fuel cells", Materials *Science Forum*, Trans Tech Publ, 613-618, (2017).

[10] M. Omrani, M. Habibi, R. Amrollahi, A. Khosravi, "Improvement of corrosion and electrical conductivity of 316L stainless steel as bipolar

plate by TiN nanoparticle implantation using plasma focus", *International Journal of Hydrogen Energy*, 37, 14676-14686, (2012).

[11] S. Karimi, N. Fraser, B. Roberts, F.R. Foulkes, "A review of metallic bipolar plates for proton exchange membrane fuel cells: materials and fabrication methods", *Advances in Materials Science and Engineering*, (2012).

[12] M.G. Fontana, Corrosion engineering, Tata McGraw-Hill Education, (2005).

[13] S.J. Peighambardoust, S. Rowshanzamir, M. Amjadi, "Review of the proton exchange membranes for fuel cell applications", *International Journal of Hydrogen Energy*, 35, 9349-9384, (2010).

[14] Y. Wang, D.O. Northwood, "An investigation into TiN-coated 316L stainless steel as a bipolar plate material for PEM fuel cells", *Journal of Power Sources*, 165, 293-298, (2007).

[15] A. Ogawa, K. Minakawa, K. Takahashi, Ti-Al-V-Mo-O alloys with an iron group element, *Google Patents*, (1994).

[16] K. Lin, X. Li, Y. Sun, X. Luo, H. Dong, "Active screen plasma nitriding of 316 stainless steel for the application of bipolar plates in proton exchange membrane fuel cells", *International Journal of Hydrogen Energy*, 39, 21470-21479, (2014).

[17] A. Ghoneim, A. Mogoda, K.A. Awad, F. Heakal, "Electrochemical studies of titanium and its Ti–6Al–4V alloy in phosphoric acid solutions", *Int. J. Electrochem. Sci*, 7, 6539-6554, (2012).

[18] B.D. Williams, K.S. Kurani, "Commercializing light-duty plug-in/plug-out hydrogen-fuel-cell vehicles: "Mobile Electricity" technologies and opportunities", *Journal of Power Sources*, 166, 549-566, (2007).

[19] V. Andreeva, V. Kazarin, The influence of the added element on the resistance to corrosion and electro-chemical behaviour of alloyed titanium, Doklady Akad. Nauk SSSR, Inst. of Physical Chemistry, Academy of Sciences, USSR, (1959).

[20] H. Tawfik, Y. Hung, D. Mahajan, "Metal bipolar plates for PEM fuel cell - a review", *Journal of Power Sources*, 163, 755-767, (2007).

[21] A. Pardo, M. Merino, A. Coy, F. Viejo, R. Arrabal, E. Matykina, "Pitting corrosion behaviour of austenitic stainless steels–combining effects of Mn and Mo additions", *Corrosion Science*, 50, 1796-1806, (2008).

[22] H.-Y. Ha, W.-G. Seo, J.Y. Park, T.-H. Lee, S. Kim, "Influences of Mo on stress corrosion cracking susceptibility of newly developed FeCrMnNiNC-based lean austenitic stainless steels", *Materials Characterization*, 119, 200-208, (2016).

[23] W. Griffiths, A. Gerrard, Y. Yue, "Oxide film defects in Al alloys and the formation of hydrogen-related porosity", IOP *Conference Series: Materials Science and Engineering, IOP Publishing*, 1-6, (2016).

[24] J. Yang, H. Yang, H. Yu, Z. Wang, X. Zeng, "Corrosion behavior of additive manufactured Ti-6Al-4V alloy in NaCl solution", *Metallurgical and Materials Transactions A*, 1-11, (2017).

[25] C.-Q. Cheng, L.-I. Klinkenberg, Y. Ise, J. Zhao, E. Tada, A. Nishikata, "Pitting corrosion of sensitised type 304 stainless steel under wet–dry cycling condition", *Corrosion Science*, 118, 217-226, (2017).